Title

Terrestrial Laser Scanner for the analysis of airport pavement geometry

Authors

Maurizio Barbarella[1], Maria Rosaria De Blasiis[2]*, Margherita Fiani[3]

[1] Department of Civil, Chemical Environmental and Materials Engineering, University of Bologna, Bologna, Italy, maurizio.barbarella@unibo.it

[2]* Corresponding Author, Department of Engineering, Roma Tre University , Roma, Italy, mariarosaria.deblasiis@uniroma3.it

[3] Department of Civil Engineering, University of Salerno , Fisciano, Italy, m.fiani@unisa.it

This is a post-peer-review, pre-copyedit version of an article published in "International Journal of Pavement Engineering". The final authenticated version is available at: https://www.tandfonline.com/doi/full/10.1080/10298436.2017.1309194

Terrestrial Laser Scanner for the analysis of airport pavement geometry

The knowledge of the geometric features of an airport's pavement surface is essential to ensuring the safety and comfort of the driving users. For this purpose, it is important to find the most suitable survey methods and computation procedures for determining these geometric features and their evolution over time. In this study, we used a terrestrial laser scanner (TLS) to survey a stretch of a taxiway of an international airport. We designed the survey with the goal of defining the optimal parameters for the scans and the spacing between the TLS station points, combining high efficiency with data quality and accuracy. An algorithm for the semi-automatic extraction of the longitudinal and transversal profiles of the track from the digital elevation model (DEM) has been implemented. Longitudinal and cross slopes have been computed from the profiles using a linear fit, assessing the conformity of the values to the standards. The algorithm allows the verification of irregularities and the assessment of the severity of deviations from a linear trend. Our approach is suitable for obtaining an accurate reconstruction of the road surface that can be measured in post-processing and that is geo-referenced in a way that allows monitoring over time. We believe that the surveying technique that we analysed and assessed could improves the effectiveness of the measurements, and it could be used wherever pavement geometry control cannot be performed on discrete elements but rather a continuous approach is needed.

Keywords: Airport pavement; pavement irregularity measurement; terrestrial laser scanner; accuracy; road surface geometry; digital elevation model; road profiles; non-destructive testing

1. Introduction

The evaluation of road pavement performance is essential for effective maintenance design. In highway and especially in airport engineering, the research is oriented towards the study of measurements that do not reduce the safety or infrastructure functionality, minimising traffic interference. Non-destructive road survey techniques meet this aim, so it is necessary to test their potential to best use their features, properly

managing the inevitable limitations that each measurement technique presents. To standardise the airport management and adjust the design and maintenance of the runways, the International Civil Aviation Organization (ICAO) has developed International Standards and Recommended Practices (SARPS) (ICAO 2013) and introduced the Safety Management System (SMS) (ICAO 2009). The Federal Aviation Administration (FAA) followed this guidance to form the SMS (FAA 2006), as did the European Aviation Safety Agency (EASA 2015).

The evaluation of the surface regularity is particularly important for the monitoring of pavement conditions to verify compliance with the minimum requirements of international standards (Lee *et al.* 2015). The paved surface of the airports must be free of irregularities that reduce adhesion conditions and cause additional stresses, leading to further progress of the damage and affecting the operational safety (Tsai *et al.* 2013). The real profile of a surface is, by its nature, continuous in space, and it includes all of the dips of the paved surface.

To measure the road geometry, various survey instruments and techniques can be used, depending on the specific characteristics to be measured (slope, roughness, dip, etc.) and the accuracy specifications. The surface characteristics can be detected by standardized tools defined as 'true profile' (Thodesen 2010). Among the static or almost-static instruments are the inclinometers and the walking profilometers, which are highly precise even if they are minimally productive (Wambold 1999). The dynamic acquisition of profile data is done through high-speed inertial profilometers (ASTM E1926 2003, Fwa et al. 2001, Karamihas et al. 2014). To use an instrument to measure the profile, the minimum variation noticeable in the output of an instrument is prescribed (LCPC 2001, Harris 2013). These instruments are the current standard for the assessment of the characteristics of the longitudinal regularity of roads at a high

speed of travel. Good performances were also achieved through the adoption of pavement evaluation field techniques, with crack laser measurement system (two 3D laser profilers) obtaining accuracy of the order of a tenth of mm, comparable with traditional measures, low productive and time consuming (Laurent et al., 2012). Florida Department of Transportation implemented a complex system based on inertial profiling tools, imagining and inertial navigation that collects simultaneously all data and computes overall pavement quality running at highway speeds (Mraz and Nazef 2008).

Surveys can also be performed with traditional topographical instruments such as total stations (TS) and digital levels. Making use of a high-precision total station and a prism mounted on a pole that is moved from one point to another, it is possible to directly obtain slopes from the surveyed points and evaluate the regularity. Cross-slope and longitudinal profiles can be also extracted from a Digital Elevation Model (DEM) built starting from the surveyed points. Although characterised by good accuracy, the survey with TS has a strong limitation due to the low density of measured points (the survey is usually performed on grid of a few meters), which affects the spatial continuity of the data surveyed. This limit does not allow the assessment of any punctual damages on the track, such as fractures and ruts, as well as localised non-conformity of the regularity of the track. The high-precision level and staff (ASTM E1364 2012) are also used for the assessment of the surface regularity and the identification of rutting. This method, although it requires a long execution time, allows the reconstruction of the slope and longitudinal profile in an absolute reference system, which is essential to study the evolution of the distress with respect to time (Tsai *et al.* 2010). In recent years, other automated survey techniques based on mobile laser systems (MLS) have also been improved to measure the road geometry (Wang *et al.*

2008, Karamanou *et al.* 2009, Pu *et al.*, 2011, Holgado-Barco *et al.* 2014), to evaluate the pavement conditions (Dondi *et al.* 2011, Aoki *et al.* 2012, Lantieri *et al.* 2015) and to estimate the slopes (Tsai *et al*. 2013), in airport context too (Aerial Data Service 2010, Riesner 2014). The main advantages that have contributed to the success of MLS are the drastic reduction in surveying times, the plurality of data acquirable, namely data from laser scans, high-resolution images, ground-penetrating radar and profilometer, and the possibility of processing the data acquired at a later time (Sukumar et al. 2006, Economou et al. 2015). The very high productivity of the MLS is not always accompanied by a high accuracy of the position of the measured points, which depends on both the measuring instruments (laser scanner, high-resolution cameras) and the navigation subsystem (GNSS, IMU, odometer). The final accuracy of the measured points to the ground downs to a few centimetres (Miller *et al.* 2012); the density of laser points is limited by the travelling speed of the vehicle and the oscillation frequency of the laser onboard. Williams *et al.* (2013) presented a review about the transportation applications of LiDAR systems comparing them with each other and highlighting some lacks in the guidelines for the use of mobile systems. Static scanning can provide some advantages over MLS, among them the higher flexibility in the choice of setup locations, the higher resolution and accuracy. A number of authors used static TLS for road survey because it appears more accurate even if less productive than the MLS (Gonzalez-Jorge *et al.* 2011, Chin and Olsen 2014). Kim *et al.* (2008) chose the static TLS for either grade or cross slope evaluation, because the mobile LiDAR is not accurate enough for highway geometric information extraction. Although MLS can be significantly more efficient than static TLS because the field time required to collect data is lesser and the vehicular interference is minimised, in airport application air

traffic flow must be interrupted anyway, whereas the higher achievable accuracy is an important requirement.

In airport context, the development of both new efficient surveying methods and new codes for the automatic extraction of the runway geometry is a current topic. Bearing in mind the technical characteristics of the latest TLS equipment, in terms of range, accuracy, point density and data acquisition rate, it could be interesting to evaluate their performance in the inspection of pavement geometry. Specific rules on the accuracy required for the measurement of slopes have not been yet adopted; there are only the prescribed acceptable threshold values. Nor is there even a regulation on surveys performed with TLS on runways. The procedure must take into account the operational context, namely the large size of the runway pavement, the need to perform fast surveys mostly at night (to minimize the interference with air traffic). Furthermore, for safety reason it is not possible materialize pillars or signals at the edges of the runway. Hence the need to use tripods and poles for setting up the instruments. When the slope value of a line is greater than a predetermined tolerance, it is necessary to determine its ground position. In the design of this specific framework, several restrictions must be respected. This leads to a number of operative choices that have a substantial influence on the achievable accuracy. The same instruments, used in different context, for example, in structural deformation monitor surveys, can provide a higher degree of accuracy (Lindberg *et al.* 2009, Pejic *et al.* 2013).

The aim of our work is to develop an operative procedure and a computational process in order to semi-automatically extract the longitudinal grade and the cross-slopes of a taxiway starting from a DEM built with TLS data. A field test was performed; the site investigated is a stretch with straight and curved sections on a taxiway of an international airport. The purpose of this study was to assess the accuracy

and feasibility of the methodology that we proposed and contribute to the realisation of standards for this type of surveys.

2. Methods

The TLS methodology for runway surveying is not yet standardised, so some operational steps and computational procedures have to be studied in detail. To survey the runway surface, at least 1800-m long and 45-60-m wide (code letter F), it is necessary to use many measuring stations and define the spacing between the TLS station points so that the survey preserves its efficiency in terms of the data quality and cost.

2.1 Single scan geometry

The actual range of the instrument mainly depends on the angle of incidence ζ (angle between the laser beam and the normal to the surface) in addition to the characteristics of the reflectivity and roughness of the scanned object. In our test case, the TLS must be placed on a tripod that, for stability, portability and operability reasons, can reach a height of about 2-2.5 m, so that the incidence angle grows very quickly with the distance of the reflection point of the beam. Its trend is shown in the left panel of Figure 1.

The received signal strength decreases with increasing incidence angle and influences the precision of the distance measure. Soudarissanane *et al.* (2009) experimentally studied the incidence angle contribution to the total error budget as $1/\cos\zeta$; Pejic *et al.* (2013) determines the maximum distance at which the error contribution due to the inclination is negligible in tunnel surveying. The spacing in the longitudinal direction between two points along the same plane of collimation increases rapidly with the distance from the station point, while the spacing in the transverse

direction (due to the horizontal angular sampling $\Delta\theta$) increases linearly, according to the trends shown in the right panel of Figure 1.

[Figure 1 near hear]

Therefore, increasing the incidence angle results both in a deteriorated signal-to-noise ratio due to elongated laser footprints on the surface, in an increase in the distances between successive footprints on pavement and in the reduction in the density of points per surface element. The points density can be computed with respect to the distance considering the vertical $\Delta\zeta$ and the horizontal $\Delta\theta$ sampling interval adopted (Lindbergh *et al.* 2009). A small $\Delta\zeta$ can lead to a superimposition of the fingerprint, and then to a blurring effect with loss of effective resolution that can be quantified via the EIFOV (Lichti and Jamtsho 2006). In the case of pavements, the density of the point cloud and the spot size varies, with regularity, in the longitudinal direction of the runway until reaching the maximum range of the instrument. Hence, it is necessary to define the threshold distance at which the resolution of the point cloud is sufficient for the purposes of the survey. Spacing between stations is thus a parameter that influences the survey efficiency. One of the aims of our study is exactly to determine the threshold distance between the scan stations.

2.2 Survey planning

The pavement surface is a long strip; it can be surveyed with a number of scans taken from a TLS placed on the axis of the runway. The distance between the stations must be chosen to ensure a high overlap between two adjacent clouds. The target to be used for registration and geo-referencing of point clouds must have the size and shape needed to enable the identification of the centroid. In our survey, we used a number of retroreflective cylinders by Riegl as tie-points and reflective spherical targets as Ground

Control Points (GCP). The targets were positioned to the side edges of the track, on the overlap area to allow an effective application of ICP algorithm in the registration phase. When registering a large sequence of scans along the runway, the propagation of uncertainty may lead to quite large errors. It is good practice to group them into blocks of few scans (i.e. six) to keep the value of the co-registration residuals low. Currently, no specific rule exists for the threshold value of the residuals. A sufficient level of accuracy of the geo-referencing process may be reached by measuring the position of the targets with RTK (Real Time Kinematic) GNSS receivers or NRTK (Network Real Time Kinematic) if it is available in the airport area. These surveying techniques enable to reach accuracy of a few cm. They are very fast and efficient, so they appear suitable for night surveys. A high-precision network to determine the position of the targets involves higher cost non compatible with the purpose of a runway maintenance survey. The survey is computed in the Reference System adopted by the airport.

2.3 Computation of profiles and slopes

Once the point clouds have been acquired, co-registered, aligned and georeferenced, a number of profiles can be extracted directly from the point clouds (Varela-Gonzales *et al.* 2014). The longitudinal profile is defined by the intersection between the road surface and a reference plane perpendicular to the surface of the pavement and parallel to the direction of travel of the lane. The transverse profile is defined by the intersection between the road surface and a reference plane perpendicular to the surface of the pavement and to the travel direction of the lane. We choose to extract the profiles directly from a grid DEM that reconstructs numerically the object because it is less expensive in terms of computation time and data storage. The generation of a numerical model of the surface of the runway allows the determination of the geometric parameters of interest, in particular the longitudinal and transverse profiles along the

section lines chosen and their grades. The chosen interpolation algorithm for constructing the grid DEM must have some characteristics: it must be fast even for very large data sets, as the point clouds contain some millions of points, it does not extrapolate z values beyond the range of data, it must avoid excessive data smoothing to be able to detect small form changes. A few algorithms, such as 'Inverse Distance Weighting', 'Natural Neighbor' and 'Linear Kriging', are all suitable for data interpolation due to the regularity of the surface. More complex is the choice of the grid step and of the search options, due to highly variable density of the cloud.

Once the DEM is built and stored, the profiles to be extracted can be chosen later in terms of number and position. To extract the profiles, a procedure implemented in MatLab has been carried out. In the first phase, the coordinates of the extremes of the runway section lines are computed. In the second phase, the profiles are computed and edited and finally their grades are estimated. The input of the first phase are the positions P_i in the absolute system of the TLS station points (surveyed on the ground). Also the values of both the distance p between subsequent section lines and their semi-length l must be given. The steps implemented are the following:

- the direction $\theta_{i,i+1}$ related to the north of each segment joining two successive points of the track axis P_i - P_{i+1} has been computed;
- intermediate points C_k with a user-defined step have been created;
- for each of them, the orientation $\theta_k=\theta_{i,i+1} + \pi/2$ of the cross-section orthogonal to the segment P_i-P_{i+1} and the coordinates of its extremes A and B at a distance l from the axis (defined by the user) have been computed.

The elevations of a series of points along the AB section, at a spacing chosen by the user, have been extracted from the grid DEM using bilinear interpolation, forming an

elevation profile corresponding to the section line AB. The implemented code consists of the following steps:

- checking that the segment AB is internal to the grid boundaries and eventually redefining the extremes inside the grid;
- computing the progressive distance d_k along the AB direction according to an increment defined by the user and determining the planimetric coordinates of the corresponding point P_k along the section;
- computing the elevation z_k of the section points through the bilinear interpolation of the elevations of the grid. The automatically generated profiles (d, z) are stored in a file.

To edit the transverse profiles and compute their grade, a second code has been written. The analyses of the profiles, especially the transverse ones, allow the identification of possible outliers, generally due to objects placed on the runways (cylinders used as tie points to co-register scans, signs, targets, etc.). To locate a section with a constant grade for each of the two slopes, the extremes of the section should be modified to ensure the isolation of the two sets of points to compute the correct slopes. For this purpose, the code ensures that:

- each elevation profile is plotted on the screen with overlapping lines indicating the position of the track axis and the extremes of the section (Figure 2(a));
- the position of the section extremes could be accepted or modified by moving the cursor (Figures 2(b) and 2(c)) to define two slopes with constant gradients (Figure 2(d));
- a least squares method is used to interpolate the points belonging to each of the two slopes to estimate the parameters of the linear regression that best fits the

section; the angular coefficient of the regression represents the grade of each slope. The standard deviations of the estimate are computed too.

For the computation of the longitudinal grades, our code computes the gradients on the stretches of the entire profile (d_k, z_k) identified with moving windows of length L, shifted from the previous section of a certain value S. The least squares method is applied in this case, too. The values of the gradients of the stretches, which are stored on Excel sheets, can then be plotted to monitor the pavement profile on any section parallel to the runway axis. The transverse grades have been computed separately for each slope.

[Figure 2 near hear]

3. Experimental survey

We carried out a TLS survey on a taxiway of an international airport. The taxiway analyzed is a flexible pavement that was deep-rehabilitated just before the date of the survey. The survey test has been performed on a short stretch of the taxiway. Figure 3 shows the station points and the positions of the targets used to georeference the four scans. A Riegl VZ400 TLS has been used for the pavement survey. The instrument of the TOF (time of flight) type is characterised by a long range, good accuracy and high-speed acquisition, and the main technical characteristics are shown in Table 1.

[Table 1 near hear]

[Figure 3 near hear]

The field measurement campaign was conducted at night, when the air traffic is reduced, to not interfere with the aircraft traffic circulation. The survey of the stretch of the taxiway was performed according to the criteria described in Section 2. With respect

to the locations of the laser stations, which are related to the taxiway geometry, the spacing between two consecutive stations has been set equal to approximately 30 m because the distances in both the longitudinal and transverse direction are almost the same, approximately 3 cm, for the angular sampling interval we used. The chosen inter-distance allows an almost symmetrical situation around the station and guarantees a significant overlap between the point clouds; nevertheless, it is considered restrictive and will be verified experimentally. The point clouds have been acquired by four station points placed on the centre line. The instrument has been set up on a dedicated tripod that is very robust and equipped with a telescopic central pole to allow raising the TLS to a height of 2.20 m. To georeference the data, a number of targets with a spherical radius of 0.15 m equipped with a stem of 0.075 m have been used. The stems have been screwed onto an adapter placed on a tribrach screwed on the tripod and put on the station at points indicated on the pavement. Each of the four scans contains from four to six targets. The targets have been placed at the edges of the track, in the positions shown in Figure 3, at a distance between 20 and 40 m from the station points. GNSS in RTK mode has been used to determine the locations of the targets. The GNSS antenna master has been mounted on a tripod placed near the survey area, while the rover antennas of the receivers have been mounted on the pole. To transform the coordinates of the vertices in the cartographic coordinate system used at the airport (the Italian National System Gauss-Boaga), the GNSS master has been connected to four vertices of known coordinates belonging to the airport frame. A precision geometric levelling starting from a benchmark inside the airport has also been performed to determine the orthometric height at the GNSS points.

The four scans acquired from the TLS, called A, B, C and D, present a strong overlapping, and each cloud contains over 20 million points. The zenith sampling

interval has been set to 0.008°, and that of the azimuth to 0.08°. Close to the targets, the scanning step is denser, to more accurately reconstruct the spherical form starting from the point cloud. Each point cloud has been georeferenced individually using the known coordinates of the targets visible in each of them. A least squares method has been used to fit the points of the cloud located on the targets (some tens of thousands) on the surface of the sphere of known radius, of which the centroid has been computed. The four clouds have also been co-registered and geo-referenced. The accuracy achieved in the definition of the spherical geometry of the target is - in terms of standard deviation - on the order of 1-2 mm. In the left panel of Table 2 we report the georeferencing accuracy of the four scans. In the right panel of the table, we report the accuracy results of the co-registration between two adjacent scans and of the global adjustment performed with an indirect registration method employing the Multi Station Adjustment (MSA) approach.

[Table 2 near hear]

4. Data processing

The outputs of the data processing are the profiles and the slopes of the taxiway. To evaluate the quality of the results obtained by TLS on airport taxiway, many tests have been performed on the acquired data. In this section, we have reported the results of the evaluations performed to choose the parameters that should be adopted for the DEM generation. The traditional survey, although characterized by a defined internal accuracy - perhaps better than TLS - cannot be used to validate the new experimental methodology because it has a lower density of points than TLS. A comparison of the profiles obtained with the two methodologies has been reported in Barbarella *et al.* (2014). Therefore, our evaluations are performed by comparing the profiles obtained on

the same section in different modes. It is very important to define the spacing between laser stations to assess the efficiency of TLS in a static mode. The spacing chosen - 30 m - can be considered conservative, used for experimentation, and it needs to be assessed in terms of its effectiveness and efficiency. The availability of a high-resolution DEM allows tracing transverse and longitudinal profiles with a very close spacing. The present paper has reported the analysis of different sections with different spacings and different distances from the station generating the point cloud. Inside the runway, it is opportune to analyse the centreline on which the central wheel of the aircraft is placed and the portion next to it on which the landing gear is placed. The longitudinal profile has been computed on the runway axis and at 3 m, (LS_{3L}, LS_{3R}), 6 m (LS_{6L}, LS_{6R}) and 10 m (LS_{10L}, LS_{10R}), on the right and left sides of the axis (Figure 3 - right panel). The transverse section TS_i has been computed at different spacings, starting from 10 m and 5 m for some comparisons until a few centimeters for the slope analysis (Figure 3 - left panel). The spacings of 5 m and 10 m have been defined in such way to approximately correspond to the stations (which are spaced every 30 m).

4.1 Procedure of georeferencing

The survey has been designed to allow the georeferencing of every single scan on the basis of only the targets present in it. It is also possible to perform the co-registration of consecutive scans. This allows identifying a single block to be georeferenced on the basis of the visible targets in the aggregated cloud. In the present analysis, both of above-mentioned methods have been implemented. To evaluate the difference between the two procedures, the profiles obtained on each intermediate section between two stations, spaced by 15 m, have been compared. In particular, the difference in height between the profiles has been computed. Figure 4 shows, as an example, the difference between the profiles obtained by scan A and scan B on section $TS_{3\text{-}4}$. The white line

represents the profile obtained after indirect georeferencing (registration of four clouds and georeferencing on the control), while the black line represents the profile obtained by direct georeferencing (georeferencing on the control). The better consistency of the white line is clear. The results suggest the opportunity to use the adjustment to obtain a better consistency of the clouds. It is nevertheless proper to split the cloud geo-referencing into several parts to limit the file size. Every single file must contain the original points of the cloud with the new orientation acquired. All of the following tests have been obtained by using the adjusted scan. The profiles could be generated directly from point clouds, but it was deemed more appropriate to extract them from the intermediate DEM grid.

[Figure 4 near hear]

4.2 Choice of the interpolation algorithm of the DEM

Many software packages allow the construction of a DEM starting from a point cloud by using different algorithms, both for realising TIN and for interpolation on GRID. The regular profile of the surface analyzed allows us to simplify the choice of interpolation algorithm. After some tests done with different algorithms, including Kriging, Radial Basis Function, Natural Neighbor, and Inverse Distance to a Power (2nd degree), we chose the last. For the step of the grid, an empirical criterion was used to select a value of the spacing between points at a medium distance from the station where the radial spacing is almost equal to the transverse spacing. Some tests were performed by setting the values of the steps of the grid equal to 2.5 cm and 10 cm using the same interpolation algorithm. To evaluate the difference between the two grid cell sizes, profiles of the same section were obtained (Figure 5). The difference in height between the two profiles has been computed, and the standard deviation σ_0 of the difference has

also been computed. The evaluation has been performed at different distances from the station and then with different inter-distances between points. In Figure 5, σ_0 has been reported, related to the distance of the section in relation to the first station (scan A); for the second one (scan B), the same trend has been observed because σ_0 lies within the range of 1 mm at a distance of tens of metres, rising up to 2 mm at one hundred metres. The results suggest that the two grid steps are equivalent for the purpose of profile analysis. In the next analyses, a spacing of 2.5 mm has been used.

[Figure 5 near hear]

4.3 Intrinsic uncertainty of profiles

To assess the intrinsic uncertainty in transverse profiles spaced at same distance from the TLS stations, a number of profiles extracted from DEM have been evaluated in terms of their difference in height. This analysis also takes into account the measurement errors in the point clouds and the approximations due to the interpolation on the grid nodes and to the construction of profiles. We have evaluated:

- three profiles spaced by 15 m from a station (on sections $TS_{3\text{-}4}$, $TS_{6\text{-}7}$, $TS_{9\text{-}10}$);
- two profiles spaced by 30 m (on sections TS_5 and TS_8); and
- one profile spaced by 45 m (on section $TS_{6\text{-}7}$).

The order of magnitude of the differences was approximately 2-3 mm for the profiles closer to the stations (approximately 10-20 m), up to twice that for the profiles 45 m away from the station. Figure 6 shows, as an example, the differences in heights (in mm) of the profiles obtained from two scans on three adjacent sections $TS_{6\text{-}7}$, TS_8 and $TS_{6\text{-}7}$ that are intermediate between stations B and C, B and D, and A and D, respectively. The trend highlighted in the graph of the central panel is probably due to

the residual disorientation of the stations compared.

[Figure 6 near hear]

4.4 Influence of the distance from the laser station on the profiles quality

Each transverse profile can be evaluated using the DEM related to the stations located at different distances from the specific profile. As example, the transverse section TS_1 (see Figure 3) can be computed using the grid derived from scan A (station located 10 m from TS_1), scan B (40 m), scan C (70 m) or scan D (100 m), and likewise for section TS_{12}. Even for the other sections intermediate between the TS_1 and TS_{12}, the distances from the stations are different depending on the scan considered. The comparison between the profiles has allowed the evaluation of the threshold distance beyond which the profiles can be considered equivalent. Figures 7 and 8 show the differences of the profiles for the extreme sections; for section TS_1 is plotted the difference of the profiles obtained from scans B, C and D compared to the profile obtained from scan A; for section TS_{12} is plotted the difference of the profiles obtained from scans A, B and C compared to that from scan D.

[Figure 7 near hear] – [Figure 8 near hear]

The comparison shows that the differences in profiles resulting from the two scans closer to the reference one have low-frequency oscillations, while the difference with the farthest scan shows high oscillations; numerically, the differences are between 10 mm and 35 mm. The spacing between the stations used in the survey allows the extraction of multiple profiles characterised by having the same distance from the laser stations. The dissimilarity between the profiles related to sections distant from the laser station compared to the profiles of the closest sections has been computed. For each difference, the standard deviation σ_0, has been computed. Figure 9 shows this parameter

depending on the distance between the compared profiles in relation to the reference one that is closer to the laser station.

[Figure 9 near hear]

The results obtained suggest that until distances of 50 m from the station, the accuracy was good, while at distances of 70-80 m, some effects that modify the real geometry of the pavement have been highlighted (σ_0 between 8 and 10 mm). The comparison of the longitudinal profiles confirms what has been observed for the transverse profiles. Figure 10 shows the difference of the profiles of the axis, extracted from the DEM by scans B, C, and D compared to the profile coming from scan A.

[Figure 10 near hear]

5. Grade computation

The international Standards ICAO (2013) require, depending on the category of 'critical aircraft', compliance with the values of the longitudinal grades and cross-slopes for all airport pavements. As an example, the maximum value prescribed for the longitudinal grade and the cross-slopes of the taxiway analysed is 1.5%. The availability of a dense DEM allows us to automatically compute, with appropriate codes, the slopes of the profiles on very close sections.

5.1 Cross slopes

The characteristics of the code implemented for the computation of the cross-slopes have been described in Section 2. In the case study, transverse sections have been determined every 0.5 m; at each section line, the transverse profiles for a 15-m width have been traced. The cross-slope has been derived by calculating the parameters of the linear fit of the profile. In addition to the computed slopes and the related error

parameters supplied by the least squares method, the code stores the coordinates of the central point of the profile located on the taxiway centreline. Therefore, it is possible to find the positions of the sections with possible outliers and to locate them on the pavement through field tracking operations. For this purpose, the cartographic coordinates of the airport system can be transformed into the corresponding coordinates of current geodetic international systems (in Europe, the proper system is ETRF2000) to identify the point of interest through tracking in Network Real Time Kinematic (NRTK) mode. If no NRTK permanent station is present near the airport, a simple RTK survey can be performed by placing the master station on a vertex of known coordinates in the airport frame. Figure 11 shows the trend of the values of the slopes as a function of the progressive distance along a stretch of the track. The graph allows easy observation as long as the normative tolerances for the cross-slopes are not exceeded.

[Figure 11 near hear]

5.2 Longitudinal grade

The implemented code also allows the extraction of the longitudinal profiles of the track. A full profile consists of a set of stretches of profiles computed using data from different scans. In this case study, it consists of two portions, the first extracted from scan A (0 to 100 m) and the second from scan D (100 to 200 m). Figure 12 shows the longitudinal profile of the taxiway axis.

[Figure 12 near hear]

We validate the grade values along a number of sections of defined length. We developed a procedure that uses a moving window of defined length and allows the computation of the grade of a segment, shifting the window of the defined length portion and calculating the grade of the new segment until the completion of the entire

track. The computed grade value is then stored for numerical analysis. Verifications both on the axis of the track and on lines on the right and left sides at distances of 3, 6 and 10 m from it have been carried out. The whole longitudinal profile has been studied on a kernel of length L = 45 m shifted to S = 10 m, by drawing a graph of the profiles and by calculating the grade using the linear regression of elevation data. Figure 13 shows the percentage values of the grades of the fifteen segments of the portion of the track surveyed. The wide overlap between adjacent windows (35 m) leads to a strong correlation between the values of the grades.

[Figure 13 near hear]

Another significant parameter computed by the code is the deviation of the points of the longitudinal profile from the 'virtual straight edge' coincident with the trend line. In Figure 14, we show the result of the calculus for a window of 45 m and the residuals of the points of the profile from the linear trend. The dashed lines identify a band of a width of 2 cm, useful to display residues larger than 1 cm in absolute value.

[Figure 14 near hear]

6. Discussion

In this paper, we proposed a survey methodology and data processing procedures based on TLS and their application to the study of an airport surface pavement. The outputs of all of the process are a number of elevation profiles extracted from a highly detailed DEM and the values of the longitudinal grade and transverse slopes. The traditional survey by the Total Station along alignments - defined at the time of the survey - allows directly obtaining profiles and slopes on the sections surveyed (Schmidt 2001). However, the points directly surveyed are at distances on the order of metres from each other and do not allow a detailed analysis of the surface.

Regarding the accuracy of the single point surveyed, the use of a Total Station does not permit obtaining better values than those obtained from a TLS. If the measurement is carried out with a direct response on the ground, the same problems of the laser scanner (discussed in Section 2) can be faced. If the measurement is done on a prism mounted on a pole, although the measurement is really precise, the defects in the vertical rod lower the accuracy of the planimetric coordinates of the point. The grade values are the outputs of the processing of the TLS data, whose process consists of multiple phases. To georeference the scans and to interpolate the data on a grid, commercial software packages should be used. For the study of the slopes and more generally the geometric characteristics of the track, we considered it most appropriate to implement a specific code. This allows us to extract from the DEM, both numerically and graphically, all of the transverse and longitudinal profiles at any time after the survey using a procedure that is substantially batch. It is not trivial to evaluate the internal uncertainty with which the profiles are derived. The comparison with the profiles derived from the survey with TS did not seem exhaustive, due to the different natures of the data surveyed. However, comparisons between some transverse profiles measured directly with TS and the corresponding profiles derived from DEM from TLS along the same section line have been carried out (Barbarella *et al*. 2014). The differences observed are sensitive, but the traditional survey with Total Station is not considered more accurate.

To achieve a significant reference, the survey with TS should be performed with particular expedients. In addition, it should have a point density greater than that which is typical to make it non-competitive. The high quantity of profiles obtained with TLS also enables a better evaluation of the actual geometry of the track, even for the control of the variation of the shape between two adjacent sections. With the aim of giving an

indication of the accuracy of the TLS method, we have analysed the profiles of the four scans, extracted along the same section lines. The differences of height of the profiles are on the order of a few millimetres, reaching a maximum of 4 mm for profiles extracted from sections 45 m away from the considered scan station. The achieved accuracy level is comparable with that obtained with the measurements with TS, with the condition of setting the laser station inter-distance to a maximum of 100 m. In the developed codes, it is possible to automatically execute the computation of the grades for the selected sections and plot the profiles. It is also possible to activate the view in graphic mode, which is time-consuming but it allows defining, in an interactive way, the stretch of section to consider for the computation of the cross-slope. This option is necessary where a counter-slope exists. In addition, the analysis of the graph allows the individuation of the areas with irregular values at which to intervene. The possibility of splitting the DEM into short intervals of the same order as the grid step shows an aspect that was much less evident for the traditional surveys, that is, the high variability of the extracted profile shapes that are used for the computation of the slopes. Figure 15 shows some cases of profiles in the sections of track with different geometries.

[Figure 15 near hear]

- Panel 1 is representative of a full super-elevated section (curve configuration);
- panels 2 and 3 are representatives of a cross-profile typical of the sections at transition curves; it is possible to note the rotation of the cross-section from a super-elevated section to a ‘normal crown’ one;
- panel 4 is representative of a ‘normal crown’ section (straight line configuration).

In all panels, it is possible to observe the stretches in the counter-slope or where the

slope rate grows, aimed at the control of outflow of the water. Looking at the examples shown in Figure 16, the need for a visual check of the sections is evident. Let us analyse in detail the presented cases.

[Figure 16 near hear]

In almost all of the cases shown, due to the pronounced irregularities of the profiles, it is wrong to represent the trend of the cross slope with an interpolating line. It is important to highlight that the problem of the ‘correctness’ of the slope values provided is not only related to the TLS survey, but is general. In fact, it is also applicable to the traditional survey, which is more discreet and therefore ‘smooths’ this aspect. Other than the slope control, which is important to guarantee the regularity of the pavement surface, the code permits the verification of the local irregularities. In fact, looking at panels 1 and 2, it is possible to note an abnormal convexity at the axis location, which is probably due to an incorrect compaction. In panels 3 and 4 on the left slope, it is possible to individuate stretches of section with no slope. In the sections shown in panels 5 and 6, note the rutting that, besides affecting the motion condition of the aircraft, provokes hydroplaning when the surface is wet. If you examine in detail the deviations from the interpolating line of the crown section trend, it is possible to measure it with good accuracy; in panel 5 you can observe that the maximum deviation from the crown section trend is equal to 2 cm in absolute value (Figure 17).

[Figure 17 near hear]

The control of close sections, allowed by the code, allows the evaluation of the condition of contact between the damaged surface and the tire.

7. Conclusions and perspectives

The use of a laser scanner in static mode, set up on points located at regular distances along the track, was found to be appropriate for the pavement survey of an airport track to evaluate its geometric features and status with good levels of accuracy (Sayers *et al.* 1986). In comparison to the traditional method based on TS, the TLS gives the same level of accuracy if it is performed with a correct operating procedure, but it provides a greater amount of data, with an almost 'continuous' characterisation of the pavement. In the analysis of the track, the availability of a dense and reliable DEM is certainly an element on the side of the TLS survey over the traditional one. The speed and the ease of surveying the road surface, along with a good level of accuracy, which is comparable with that achievable with traditional measurements, are important inputs to suppose a reliable quality control during the progress of works compared to the traditional method. However, although the effort on the field for the TLS survey is similar to that required for the traditional survey, the processing is more complex, and it is necessary to follow a careful procedure for the georeferencing of the clouds of laser points for the creation of the DEM and its analysis.

For practical applications, it is convenient to use codes implemented ad hoc that allow the semi-automatic generation of section lines and profiles and the computation of the gradients. To evaluate both the accuracy level of single transverse profiles and the worsening of the accuracy of the measurements upon increasing the distance from the laser station, an internal comparison of the results of different scans on the same section is considered because the direct survey with TS cannot be considered as a comparison term with respect to the laser method. In the light of the testing carried out, to obtain good results, it is necessary to

- execute the block adjustment of the scans acquired to obtain the maximum congruence of the clouds upon the correct placement of targets in the reference frame of the airport;
- set up the TLS instrument in the highest possible position, compatible with the stability because the range and the quality of the single point depends on the inclination angle, and other parameters depend on the characteristics of the pavement (roughness, reflectance, etc.);
- set up the TLS station points to a maximum distance of 100 m from each other.

The analysis of the numeric values of the slopes that are computed by the developed code allows controlling if they are inside the limits of the standard requirements of the airport. The control of the longitudinal profiles at the track axis and in the areas occupied by the landing gears of the aircraft can also be performed in an automatic manner. The good results achievable by the terrestrial laser scanner in static mode, both in terms of the accuracy and the control of the detailed and general aspects of the track, can induce a review of the control techniques that are actually used to define the conformity to standards. Therefore, the laser scanner method could not be only allowed, but actually recommended as a surveying method.

The technique analysed in the present paper critically improves the quality of the measurements, and it can be used wherever the pavement control of the track cannot be performed on discrete elements but rather requires a continuous surface. This is the case, for example, for the control of the superficial regularity. Among the future developments of the experimentation, there is the examination of the contribution of the TLS survey for the computation of the parameters indicative of regularity. Finally, in our opinion, if this surveying technique will be considered as an alternative method to

the traditional one, it is important to prepare new standards that take into account all of the features of the laser data.

Disclosure statement

No potential conflict of interest was reported by the authors.

References

Aerial Data Service, 2010. Meacham International Airport (KFTW), Runway 17/35: Mobile Mapping Runway Profile Demonstration. Available from: http://www.industrycortex.com/datasheets/profile/1000391564/meacham-international-airport-kftw-runway-1735-mobile-mapping.

Aoki, K., Yamamoto, K. and Shimamura, H., 2012. Evaluation Model For Pavement Surface Distress On 3d Point Clouds From Mobile Mapping System. In: Int. Arch. Photogramm. Remote Sens. Spatial Inf. Sci., XXXIX-B3. XXII ISPRS Congress, 25 August – 1 September 2012, Melbourne, Australia, 87-90.

ASTM E1364. 2012. Standard Test Method for Measuring Road Roughness by Static Level Method. American Society for Testing and Materials. Available from: www.astm.org.

ASTM E1926, 2003. Standard practice for computing international roughness index of road from longitudinal profile measurement. American Society for Testing and Materials. Available from: www.astm.org.

Barbarella, M., De Blasiis, M.R., Fiani, M., Santoni, M., 2014. A LiDAR application to the study of taxiway surface evenness and slope. In: ISPRS Ann. Photogramm. Remote Sens. Spatial Inf. Sci., II-5. 2014 ISPRS Technical Commission V Symposium, 23 – 25 June 2014, Riva del Garda, Italy, 65-72.

Chin, A. and Olsen, M., 2014. Evaluation of Technologies for Road Profile Capture, Analysis, and Evaluation. J. Surv. Eng., 141(1), 1–13.

Dondi, G., Barbarella, M., Sangiorgi, C., Lantieri, C., De Marco, L., 2011. A semi-authomatic methodology to identify defects on a road surface. In: Proceedings of the International Conference on Sustainable Design and Construction 2011, Kansas City, Missouri, 704-711.

EASA, 2015. Certification Specifications and Guidance Material for Aerodromes Design CS-ADR-DSN - Annex to ED Decision 2015/001/R. European Aviation Safety Agency, 225.

Economou, N., Vafidis A., Benedetto, F., Alani, A.M., 2015. GPR Data Processing Techniques. In: Benedetto, A. and Pajewski, L. eds. Civil Engineering Applications of Ground Penetrating Radar. Springer Transactions in Civil and Environmental Engineering, 281-297.

FAA, 2006. Airport pavement management program AC n.150/5380-7A. Washington, DC: Federal Aviation Administration U.S. Department of Transportation.

Fwa, T.F., Nixon, E. and Chan, W.T., 2001. Multi-Year Pavement Management Programming For Road Network. Journal of the Eastern Asia Society for Transportation Studies, 4 (1), 423-433.

Gonzalez-Jorge H., Riveiro, B., Armesto, J.,Arias, P., 2011. Standard artifact for the geometric verification of terrestrial laser scanning systems, Optics & Laser Technology, 43(7), 1249 - 1256.

Harris, D., 2013. Development of Methods and Specifications for the Use of Inertial Profilers and the International Roughness Index for Newly Constructed Pavement. Publication FHWA/IN/JTRP-2013/09. Joint Transportation Research Program. West Lafayette, IN: Indiana Department of Transportation and Purdue University.

Holgado-Barco, A., Gonzalez-Aguilera, D., Arias-Sanchez, P., Martinez-Sanchez, J., 2014. An automated approach to vertical road characterisation using mobile LiDAR systems: Longitudinal profiles and cross-sections. ISPRS Journal of Photogrammetry and Remote Sensing, 96, 28-37.

ICAO, 2009. Safety management manual, Doc 9859. 2nd ed. Montréal: International Civil Aviation Organization.

ICAO, 2013. Annex 14, Vol I – aerodrome design and operations. 6th ed. Montréal: International Civil Aviation Organization.

Karamanou, A., Papazissi, K., Paradissis, D., Psarianos, B., 2009. Precise estimation of road horizontal and vertical geometric features using mobile mapping techniques. Bol. Ciênc. Geod. Special Issue on Mobile Mapping Technology 15(5), 762-775.

Karamihas, S.M., Barnes, M. A. and Rasmussen, R.O., 2014. Pavement surface specification for road load measurement. Report of University of Michigan, Transportation Research Institute (UMTRI), 2014-2019. Ann Harbor, MI, 1–43.

Kim, J.S.; Lee, J.C.; Kang, I.J.; Cha, S.Y.; Choi, H.; Lee, T.G., 2008. Extraction of geometric information on highway using terrestrial laser scanning technology. International Archives of the Photogrammetry, Remote Sensing and Spatial Information Sciences. 37 (B5), 539–544.

Lantieri, C., Lamperti, R., Simone, A., Vignali, V., Sangiorgi, C., Dondi, G., 2015. Mobile Laser Scanning System for Assessment of the Rainwater Runoff and

Drainage Conditions on Road Pavements. International Journal of Pavement Research and Technology, 8(1), 1-9.

Laurent, J., et al., 2012. Using 3D laser road profiling sensors for the automated measurement of road surface conditions. In: Scarpas, A., Kringos, N., Al-Qadi, I., A., eds., 7th RILEM international conference on cracking in pavements, mechanisms, modeling, testing, detection and prevention case histories, Vol. 4, 2012. Dordrecht: Springer, 157–167.

LCPC, 2001. Mesure et interpretation du profil en travers, Methode d'essai n. 49, Techniques et methods des laboratoires des ponts et chaussées. Laboratoire central des ponts et chaussées (LCPC) Eds.

Lee, J., Nam, B. and Abdel-Aty, M., 2015. Effects of pavement surface conditions on traffic crash severity. Journal of Transportation Engineering, 141 (10), 1–11. doi:10.1061/(ASCE)TE.1943-q5436.0000785,04015020.

Lichti, D.D. and Jamtsho, S., 2006. Angular Resolution of Terrestrial Laser Scanners, The Photogrammetric Record, 21(114), 141-160.

Lindberg R.C., Uchananski L, Bucksch, A., van Gonslinga R., 2009, Structural monitoring of tunnels using terrestrial laser scanning. Reports of Geodesy, 2(87): 231-23

Miller, N., Brian, S. and Nicholson, K., 2012. A Comparison of Mobile Scanning to a Total Station Survey at the I-35 and IA 92 Interchange in Warren County, Iowa. Final Report August 15, 2012, Project RB22-011. Iowa Department of Transportation and the Federal Highway Administration, Ames, IA.

Mraz, A., and Nazef, A., 2008. Innovative Techniques with a Multipurpose Survey Vehicle for Automated Analysis of Cross-Slope Data. Transportation Research Record: Journal of the Transportation Research Board, No. 2068. Washington, DC: Transportation Research Board of the National Academies, 32–38.

Pejic, M., *et al.*, 2013. Design and optimisation of laser scanning for tunnels geometry inspection. Tunnelling and Underground Space Technology, 37 (37), 199–206.

Pu, S., *et al.*, 2011. Recognizing basic structures from mobile laser scanning data for road inventory studies. ISPRS Journal of Photogrammetry and Remote Sensing, Supplement Advances in LIDAR Data Processing and Applications, 66, 28-39. Available from: http://www.sciencedirect.com/science/article/pii/S0924271611000955

Riesner, E. 2014. Modern Airfield Pavement Management Strategies. The 2014 airports conference, 3–5 March 2014. Hershey, PA.

Sayers, M., Gillespie, T. and Paterson, D., 1986. Guidelines for the conduct and calibration of Road Roughness Measurements. World Bank Technical Paper, 46, World Bank, Washington, D.C.

Schmidt, B., 2001. EVEN Project, Experiment to Compare and Harmonize Methods for Assessment of Longitudinal and Transverse Evenness of Pavement. Transportation Research Record, 1764, 221-231.

Soudarissanane, S., Lindenbergh, R., Menenti, M., and Teunissen, P. (2009). Incidence angle influence on the quality of terrestrial laser scanning points. In Proceedings of the ISPRS Workshop, Laser Scanning 2009, (38), 183–188

Sukumar, S.R., Yu, S., Page, D.L., Koschan, A.F., Abidi, M.A., 2006. Multi-sensor Integration for Unmanned Terrain Modeling. In: Proc. SPIE Unmanned Systems Technology VIII, 17 April 2006, Orlando, FL, 6230, 65-74.

Thodesen, C.C., 2010. SIP Project: State of the art study of infrastructure evaluation procedures for road pavements, and railway tracks. SINTEF Report SBF IN A10009.

Tsai, Y., *et al.*, 2010. Horizontal Roadway Curvature Computation Algorithm Using Vision Technology. Computer-Aided Civil and Infrastructure Engineering, 25, 78–88.

Tsai, Y., *et al.*, 2013. A mobile cross slope measurement method using LiDAR technology. Transportation Research Record, 2367, 53-59.

Varela-González, M., et al., 2014. Automatic filtering of vehicles from mobile LiDAR datasets. Measurement, 53 (2014), 215–223.

Wambold, J. C., 1999. State of the art of measurement and analysis of road roughness. Transportation Research Record, 836, 21-29.

Wang C., *et al.*, 2008. Automatic road vector extraction for mobile mapping systems. In: Int. Arch. Photogramm. Remote Sens. Spatial Inf. Sci., XXXVII-B3, XXI ISPRS Congress, 3 - 11 July 2008, Beijing, China, 515-521.

Williams, K., *et al.*, 2013 Synthesis of transportation applications of mobile LiDAR. Remote Sens. 5 (9), 4652–4692. Available from: http://www.mdpi.com/2072-4292/5/9/4652

Max. range	350/600 m (high speed/long-range mode)
Min. Horiz. & Vert. step size	0.0024°
Beam divergence	0.3 mrad
Beam diameter at exit	7 mm
Spot at 50 m distance	18 mm
Uncertainty of Horiz. & Vert. Step size	0.0034°
Max. measurement rate (kHz)	300

Table 1. Riegl VZ-400 technical characteristics.

Scan	A	B	C	D	D-C	B-C	A-BCD	Global adj.
# used targets	6	6	6	4	4	6	4	6
Standard deviation	3.9	5.5	5.4	6.4	1.4	1.8	1.4	29.9
Radial mean deviation	1.8	4.1	6.0	3.0	0.4	0.8	1.4	4.5
Mean deviation θ	-0.1	-0.2	-0.2	-0.1	0	0	-0.1	-0.1
Mean deviation ϕ	-0.2	0.1	0.2	0.3	0	0	-0.1	0.4

Table 2. Left panel: georeferencing accuracy of the four scans results (mm). Right panel: accuracy of the co-registration between scans and global adjustment accuracy (mm).

Figure 1. Left panel: inclination angle of the laser beam axis on the pavement surface as function of the distance. Right panel: distance between the laser points in the longitudinal way (continuous line) and transversal way (dashed line); horizontal angular sampling $\Delta\theta$=0.1° and vertical $\Delta\theta$=0.01°

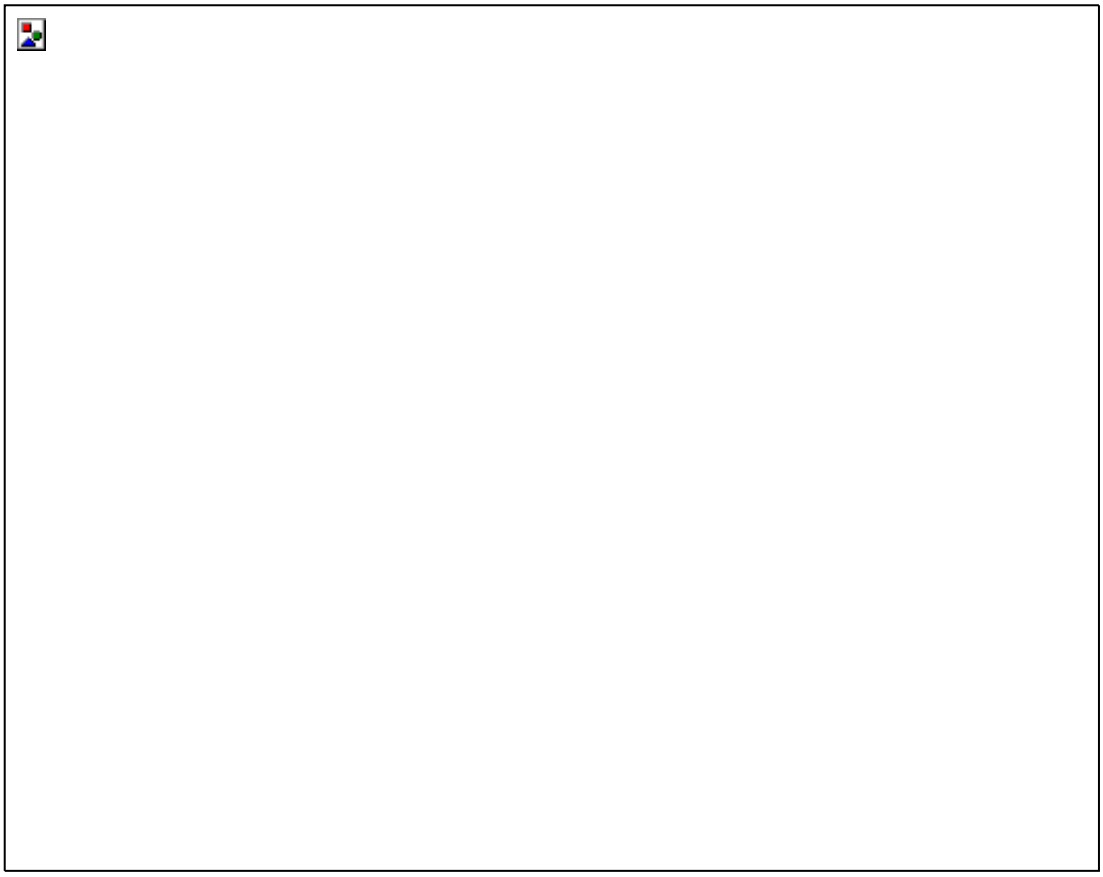

Figure 2. Choice of the border points that define the slope. (a) Profile extracted from the grid DEM; (b) shift of the left extreme to remove the points belonging to a target from

the data-set; (c) shift of the right extreme to remove a counter-slope stretch; (d) proper definition of the extremes of the slope.

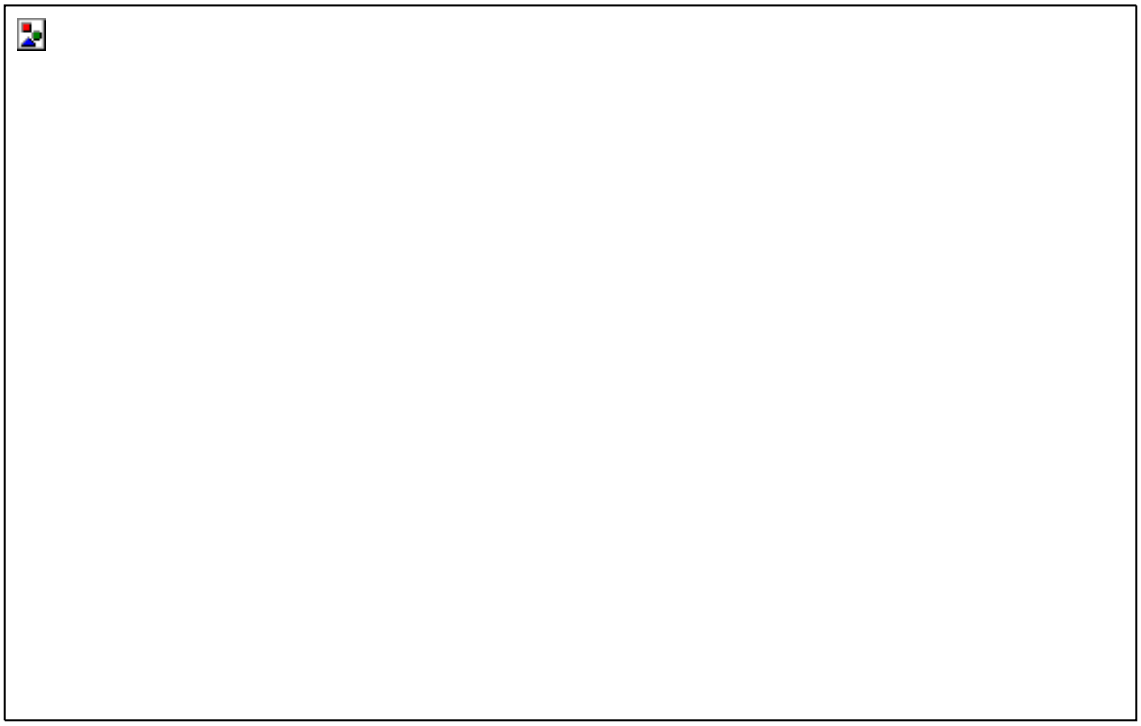

Figure 3. TLS Survey scheme. Left panel: the transversal sections (TS) every 10 m, right panel: the longitudinal sections (LS) 3, 6 m and 10 m at left and right of the centre line.

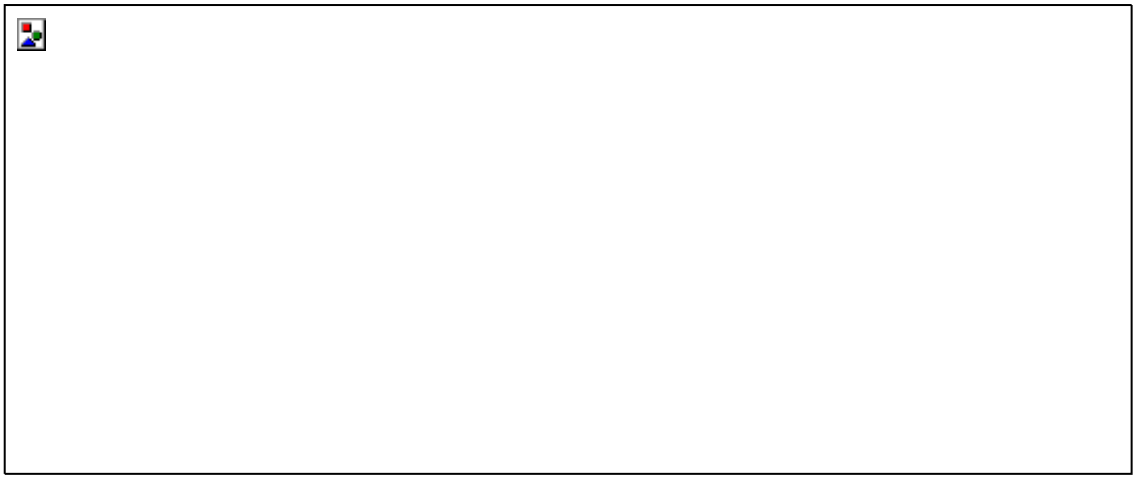

Figure 4. Difference between the profiles extracted from scans A and B on the section TS3–4 (15 m away from both the scans).

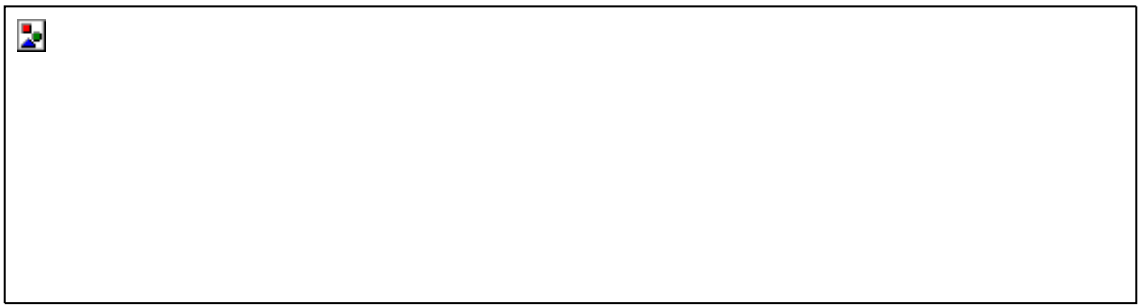

Figure 5. Comparison between DEMs with different grid cell size. The graphs show the value of the standard deviations of the height differences between the profiles extracted from the grid of step 10 and 2.5 cm, depending on the distance of the sections from the station. Left panel: point cloud acquired from the station point A; right panel: point cloud acquired from the station point B.

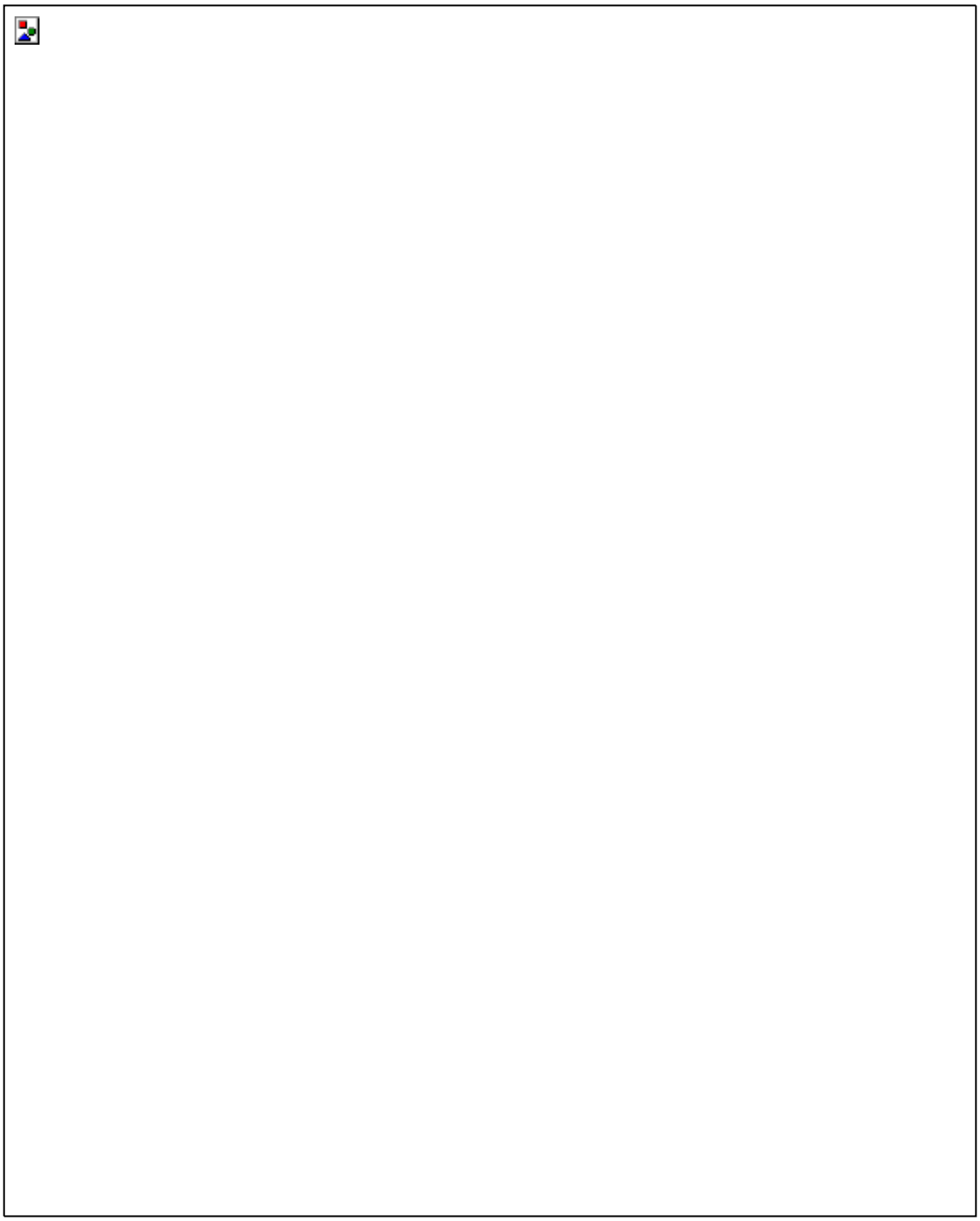

Figure 6. Differences in heights between the profiles extracted from the scans on a section located at the same distance (15/30/45 m) from the laser stations. Top panel: section $TS_{6\text{-}7}$; central panel: section TS_{8}; bottom panel: section $TS_{6\text{-}7}$.

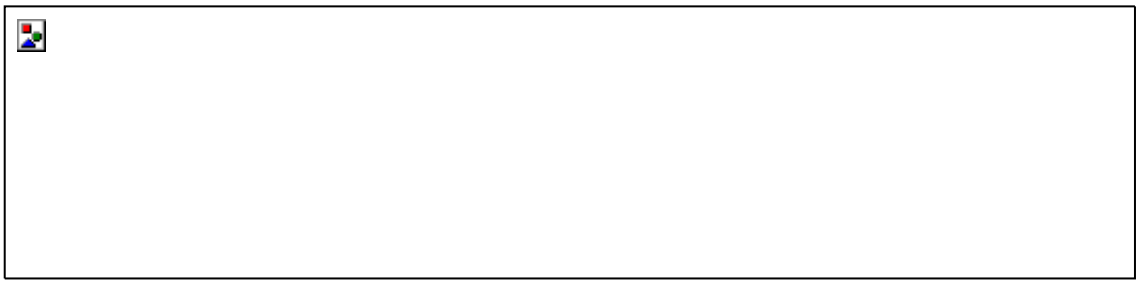

Figure 7. Transversal section 1: Differences of the profiles extracted from the scans B, C and D compared to the one extracted from scan A (at 10 m).

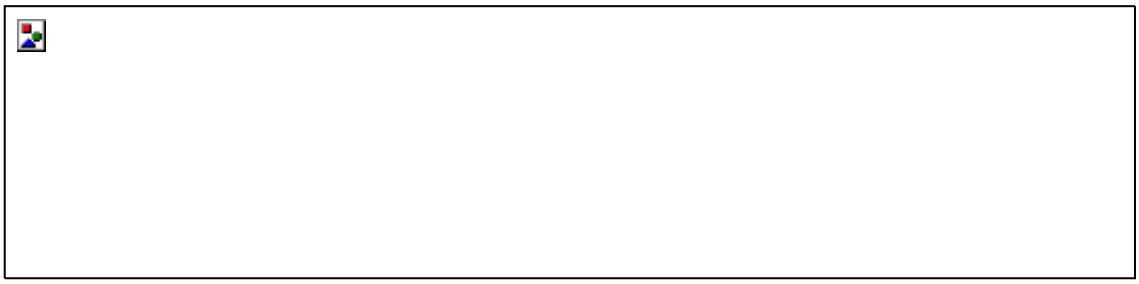

Figure 8. Transversal section12: Differences of the profiles obtained from the scans C, B and A compared to the one extracted from scan D (at 10 m).

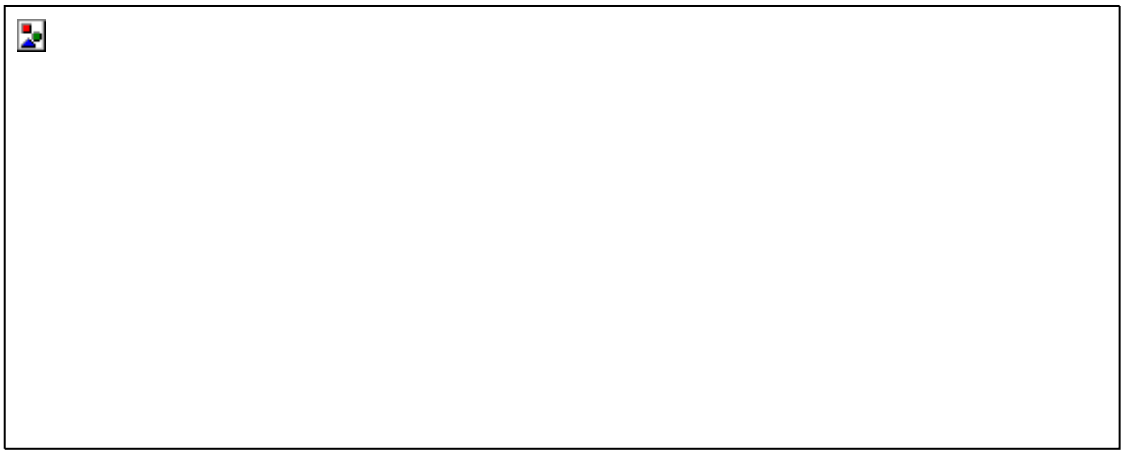

Figure 9. Rms of the height differences between far and close profiles, depending on the distance. In the right panel, the σ0 related to the same distances have been averaged.

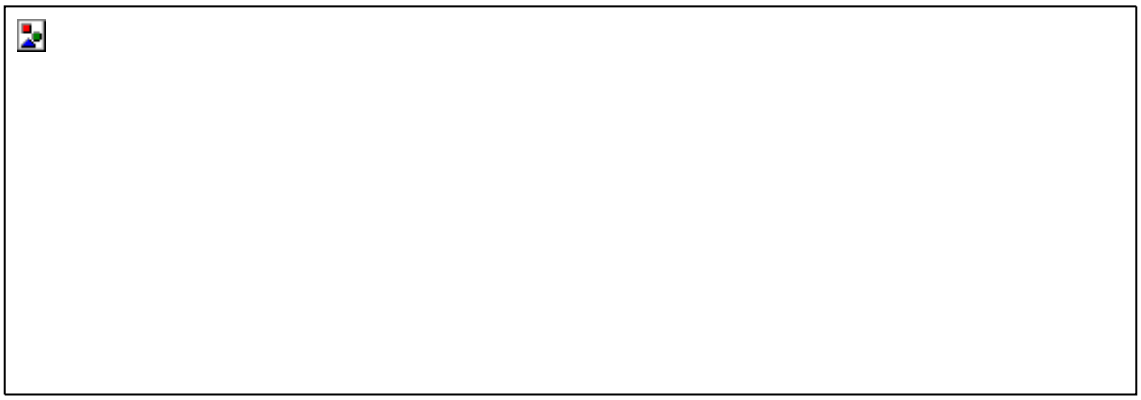

Figure 10. Differences between the longitudinal profiles of the taxiway axis extracted from the scans B, C and D (30, 60, 90 m away from A), compared to the profile obtained by the scan A.

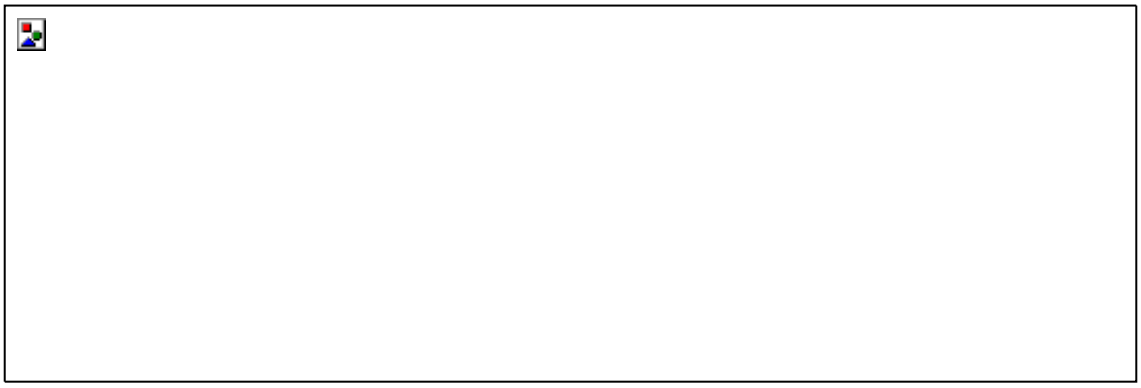

Figure 11. Trend of the values of the slopes of the transversal profile traced every 0.5 m along the taxiway, depending on their distance. Dotted line: the left part of the crown section; continuous line: the right part of the crown section.

Figure 12. Longitudinal profile of the taxiway.

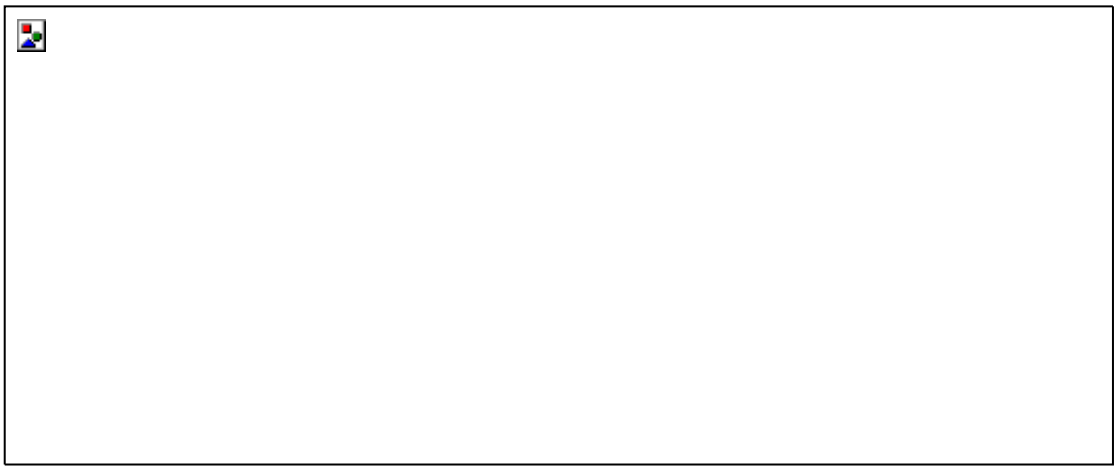

Figure 13. The percentage value of the slopes of the stretches included in the 15 kernels of length L = 45 m.

Figure 14. Left panel: longitudinal profile and cross slope for stretch of 45 m; right panel: residuals of the points of the profile from the linear trend.

Figure 15. Left panel: a shaded relief map of the grid DEM; the dots are the extremes of the cross section lines traced every 10 m. Right panels: some characteristic profiles extracted corresponding to the section lines traced on the left panel.

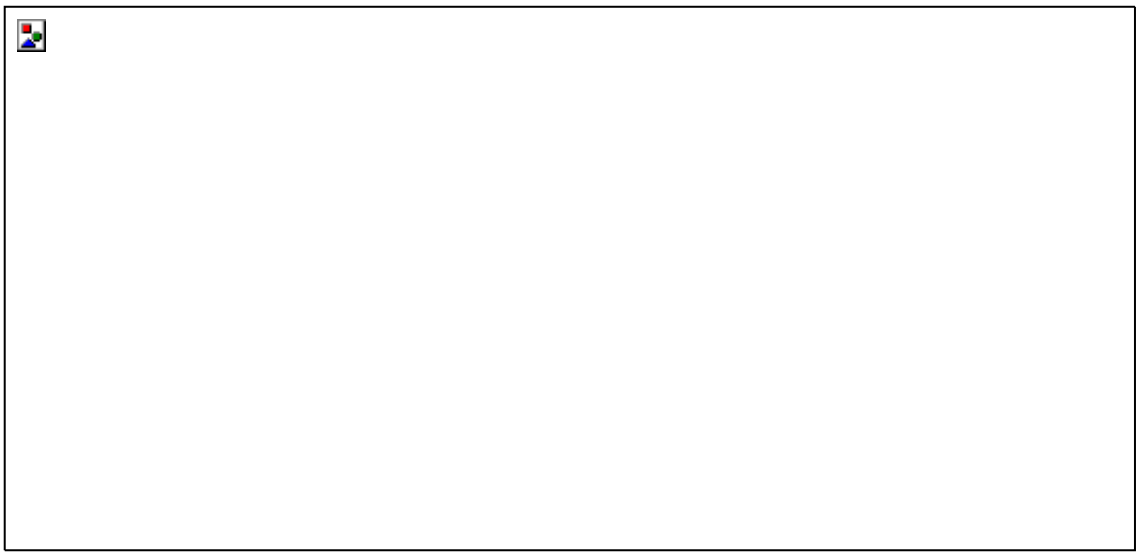

Figure 16. Examples of transversal profiles of the taxiway.

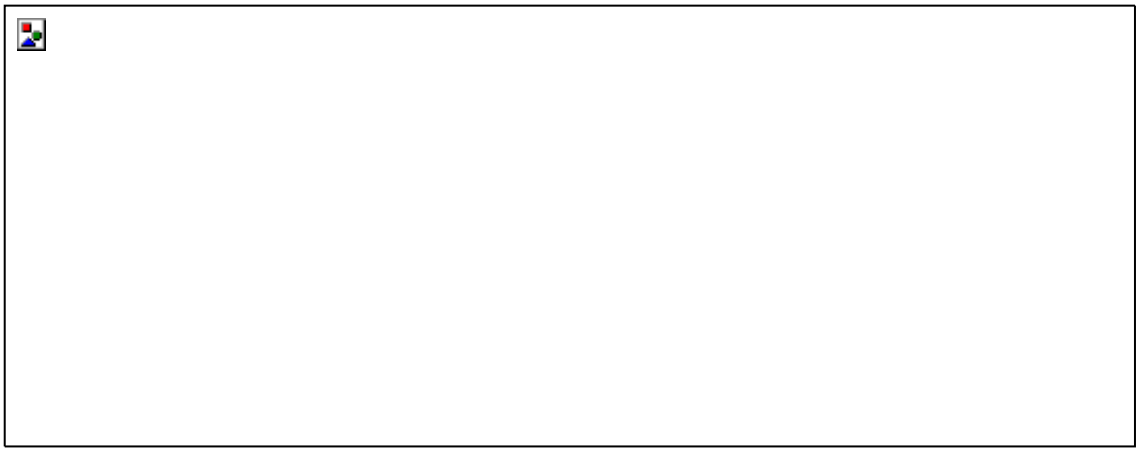

Figure 17. Left and right slopes of the transversal section n.16 shown in Figure 15. Profile slope and residuals from the interpolating line.